Topic Introduction

Voltage-Sensitive Dye Imaging of Neocortical Activity

Amiram Grinvald, David B. Omer, Dahlia Sharon, Ivo Vanzetta, and Rina Hildesheim

Neural computations underlying sensory perception, cognition, and motor control are performed by populations of neurons at different anatomical and temporal scales. Few techniques are currently available for exploring the dynamics of local and large range populations. Voltage-sensitive dye imaging (VSDI), based on organic voltage probes, reveals neural population activity in areas ranging from a few tens of micrometers to a couple of centimeters, or two areas up to ~10 cm apart. VSDI provides a submillisecond temporal resolution and a spatial resolution of ~50 μm. The dye signal emphasizes subthreshold synaptic potentials. VSDI has been applied in the mouse, rat, gerbil, ferret, tree shrew, cat, and monkey cortices to explore the lateral spread of retinotopic or somatotopic activation; the dynamic spatiotemporal pattern resulting from sensory activation, including the somatosensory, olfactory, auditory, and visual modalities; and motor preparation and the properties of spontaneously occurring population activity. In this introduction, we focus on VSDI in vivo and review results obtained mostly in the visual system in our laboratory.

INTRODUCTION

The activity of highly distributed neural networks is thought to underlie sensory processing, motor coordination, and higher brain functions. These intricate networks are composed of large numbers of individual neurons, which interact through synaptic connections in complex, dynamically regulated spatiotemporal patterns. To understand network properties and functions, it is helpful to study the ensemble activity of neuronal populations, because coherent activity of many neurons is often responsible for performing the function rather than individual cells. Functionally related subnetworks of neurons are often spatially segregated, making imaging techniques ideal for monitoring population activity. Our understanding of the contribution of single neurons for generating percepts and controlling behavior can be improved within the context of the relationship between single-cell-level and population-level activity.

The remarkable performance of the mammalian brain largely arises from computations taking place in the neocortex. The neocortex is organized into cortical columns (Mountcastle 1957; Hubel and Wiesel 1962), which have lateral dimensions of a few hundred micrometers. Interactions within and between cortical columns occur on the timescale of milliseconds. To follow neuronal computations at the fundamental level of cortical columns in real time, therefore, requires a spatial resolution of ~100 μm and a temporal resolution of ~1 msec. In vivo voltage-sensitive dye imaging (VSDI) (Grinvald et al. 1984; Orbach et al. 1985) fulfills these technical requirements and should help resolve many fundamental questions.

Electrical communication in cortical networks comprises two basic signals: subthreshold potentials (reflecting synaptic input onto dendrites) and suprathreshold action potentials (forming the

Adapted from *Imaging in Neuroscience: A Laboratory Manual* (ed. Helmchen and Konnerth). CSHL Press, Cold Spring Harbor, NY, USA, 2011.

Cite this introduction as *Cold Spring Harb Protoc*; doi:10.1101/pdb.top089367

neuronal output). VSDI appears to relate primarily to spatiotemporal patterns of the subthreshold synaptically driven membrane potentials simply because of the relatively larger area of neocortical dendrites. Therefore, VSDI allows for monitoring of the fluctuations of the membrane potential of the population away from and toward the threshold for action potential. Single unit and multiunit recordings cannot monitor this activity, reflecting only spiking activity. The local field potential (LFP), which reflects synaptic potentials, changes its polarity depending on the activity source, and therefore provides ambiguous information about the sign of recorded activity (inhibition vs. excitation). Furthermore, its spatial resolution is far lower. Therefore, VSDI has a unique place among available techniques for measuring neural activity.

Here, we describe how in vivo VSDI (Grinvald et al. 1984; Shoham et al. 1999; Grinvald and Hildesheim 2004) can be applied to anesthetized mammals as well as awake behaving monkeys. We describe previous findings and technical advances, mostly from our laboratory, and how VSDI has been combined with intracortical microstimulation, single-unit recording, local-field-potential recording, and targeted injections. We conclude by discussing further technical developments to overcome current limitations. This introduction begins by reviewing methodology and historical aspects of in vivo VSDI. To provide the reader with a sense for what type of questions may be resolved by this technique, we proceed by discussing results obtained in a variety of mammalian species and paradigms, from sensory cortex of anesthetized rats and cats to motor cortex of behaving monkeys performed in our laboratory.

FROM IN VITRO SINGLE-CELL RECORDINGS TO IN VIVO POPULATION IMAGING

To perform optical imaging of electrical activity, the preparation under study is first stained with a suitable voltage-sensitive dye. The dye molecules bind to the external surface of excitable membranes and act as molecular transducers that transform any changes in membrane potential into optical signals. These optical signals are observed as changes in absorption or emitted fluorescence, and they respond to membrane potential changes in microseconds. The voltage-sensitive dye signals are linearly correlated with both the membrane potential changes and the membrane area of the stained neuronal elements. These optical changes are monitored with light-imaging devices positioned in a microscope image plane. Optical signals using voltage-sensitive dyes were first recorded by Tasaki et al. (1968) in the squid giant axon, and by Cohen and his colleagues in the squid giant axon and in individual leech neurons (Salzberg et al. 1973).

VSDI (multiple pixels), as opposed to optical recording (single pixel rather than a full image), began with photodiode arrays in invertebrate ganglia (Grinvald et al. 1981) and was subsequently used in mammalian brain slices (Grinvald et al. 1982a) and in the isolated salamander olfactory bulb (Orbach and Cohen 1983). These initial results suggested that optical imaging could be a useful tool with which to study the mammalian brain in vivo as well. However, the initial in vivo experiments in rat visual cortex in 1982 revealed several complications that had to be overcome. One complication was the large amount of noise caused by respiratory and heartbeat pulsation. In addition, the relative opacity and packing density of the cortex limited the penetration of the excitation light and the ability of dyes to stain deep layers of the cortex. Subsequently, new, improved dyes that overcame these problems were developed (e.g., RH-414; Grinvald et al. 1982b), and an effective remedy for the heartbeat noise was found by synchronizing data acquisition with the electrocardiogram and subtracting a no-stimulus trial. These improvements facilitated in vivo imaging of several different sensory systems, including the retinotopic responses in the frog optic tectum (Grinvald et al. 1984), the whisker barrels in rat somatosensory cortex (Orbach et al. 1985), and experiments on the salamander olfactory bulb (Kauer et al. 1987; Kauer 1988; Cinelli and Kauer 1995; Cinelli et al. 1995). The development of more hydrophilic dyes improved the quality of the results obtained in cat and monkey visual cortex (e.g., RH-704 and RH-795; Grinvald et al. 1986, 1994).

The newest generation of voltage-sensitive dyes offers a 30-fold improvement in signal-to-noise ratio (SNR) over the early dyes. This was accomplished by designing dyes that are excited outside the absorption band of hemoglobin, thus minimizing pulsation and hemodynamic noise (Shoham et al.

 Cite this introduction as *Cold Spring Harb Protoc;* doi:10.1101/pdb.top089367

1999). With this advance it has become possible to reveal the dynamics of cortical information processing and its underlying functional architecture at the necessary spatial and temporal resolution in both anesthetized and behaving animals. Additional advances related to the implantation of transparent artificial dura (Arieli et al. 2002) now allow chronic recordings to be taken over a long period of time. Optical imaging can be performed simultaneously with intracellular recording, extracellular recording, microstimulation, and tracer injection, thanks to the development of an electrode assembly attached to a cranial window (Arieli and Grinvald 2002).

It is important to comment on the relationship between the in vivo dye population signal and membrane potential changes. In simpler preparations, where single cells are distinctly visible, the dye signal looks just like an intracellular electrical recording (Salzberg et al. 1973, 1977; Grinvald et al. 1977, 1981, 1982b). In optical imaging from cortical tissue stained by topical application, however, the optical signal does not have single-cell resolution. Rather, it likely represents the sum of membrane potential changes in both presynaptic and postsynaptic neuronal elements, as well as a possible contribution from the depolarization of neighboring glial cells (Konnerth and Orkand 1986; Lev-Ram and Grinvald 1986). Because of the much larger area of dendrites relative to that of cell somata (~1000-fold), the voltage-sensitive dye signal in cortical tissue reflects, in the main, the postsynaptic potentials in the fine dendrites of cortical cells, rather than action potentials in cell somata. VSDI can therefore easily detect subthreshold synaptic potentials in the extensive dendritic arborization. Recent patch recordings from the rat somatosensory cortex, performed simultaneously with VSDI, indicated that the signals originate primarily from layers 2/3 and reflect dendritic postsynaptic potentials rather than somatic action potentials (Sterkin et al. 1998; Petersen et al. 2003a). Thus, dye signals are uniquely poised to supply data about subthreshold dendritic processing, providing information about aspects of neuronal processing that cannot usually be obtained from single-unit recordings or intracellular somatic recordings.

SPATIAL AND TEMPORAL RESOLUTION

Early VSDI used a cumbersome and low-resolution 12×12 "diode array camera" (Grinvald et al. 1981). Higher resolution has subsequently been achieved, due mostly to efforts by two groups in Japan: Kamino (Hirota et al. 1995) and Matsumoto (Iijima et al. 1992; Vranesic et al. 1994). Further increases in spatial resolution were achieved by Toyama and colleagues using a stroboscopic light (Toyama and Tanifuji 1991; Tanifuji et al. 1993). Today, commercial voltage-sensitive dye cameras (charge-coupled device [CCD] or complementary metal oxide semiconductor [CMOS]), with up to 1,000,000 detectors, are available from several vendors.

Detector technology, however, is not the factor that currently limits the spatial resolution achieved with VSDI. The properties of the dyes are a major limiting factor; in particular, the SNR that can be obtained with them, and the photodynamic damage that they cause. The development of suitable voltage-sensitive dyes is a key to the successful application of optical imaging for several reasons. First, different preparations often require dyes with different properties (Ross and Reichardt 1979; Cohen and Lesher 1986; Grinvald et al. 1988). Recently, it was shown that even within the same species, different cortical areas require different dyes (e.g., a given dye provided a high-quality signal in the rat somatosensory cortex but not in the rat olfactory bulb, although the bulb was well stained [Spors and Grinvald 2002]). Second, the use of dyes is associated with difficulties that must be overcome. Under prolonged or intense illumination, dyes cause photodynamic damage. Additional difficulties include bleaching, limited depth of penetration into the cortex, and possible pharmacological side effects.

However, recent intracellular recordings in vivo have directly confirmed that stained cortical cells maintain their response properties (Sterkin et al. 1998; Grinvald et al. 1999, Fig. 23; Petersen et al. 2003a). Furthermore, long-term VSDI in awake monkeys indicated that, even after a year of imaging, monkey visual cortex continues to function normally: The animal maintained normal performance in tasks that required the cortical area be monitored. Thus, new dyes (Shoham et al. 1999) have largely alleviated the problems of pharmacological side effects and photodynamic damage. This means that

extensive imaging sessions are now possible, allowing signal averaging of many repeated presentations and improved SNRs, thus enhancing spatial resolution.

An additional factor that determines spatial resolution of VSDI is the structure of the cellular elements giving rise to the dye signal. Because the local dendritic trees of neurons have a diameter of ~300–500 μm, a given pixel combines activity from cells with distant somas. Because dendritic trees of neurons, tuned to different functional properties, overlap only partially, subdendrite resolution is possible. The temporal resolution of VSDI is not limited by the response time of dye molecules, because these respond within microseconds to a change in the electrical field over the membrane (Cohen et al. 1974). The temporal resolution is, however, limited by the nature of the population activity and the SNR. The power spectrum of other forms of population activity (electroencephalogram and LFP) suggests that most of the signal does not require a temporal resolution of >5–10 msec. Achieving high SNRs depends largely, as explained above, on the dyes used and is somewhat more demanding in VSDI than in the sister technology of intrinsic imaging because the samples are shorter in time. This is because of the square-root relationship between the number of samples and the SNR. It is much easier to obtain a good SNR when signals are slower. For instance, the SNR in measurements of small signals is 33-fold higher when the signals have a rise time of 1 sec, when compared with a rise time of 1 msec.

Empirically, we find that current dyes and equipment allow excellent SNR at a sampling rate of 5–10 msec with each pixel looking at a 64 × 64-μm area of cortex. Finer temporal and spatial sampling does not usually provide additional data, although exceptions do exist as noted in the study of the lateral spread beyond the retinotopic border, when a sampling rate of 0.6 msec was used (Derdikman et al. 2003; Petersen et al. 2003a,b). VSDI has been said to kill spatial resolution to gain better temporal resolution. The above numbers actually show, however, that no such trade-off exists with the present state of the art, relative to intrinsic imaging. Improvements in the dyes and in the spatial resolution of fast cameras have made it possible to obtain high-resolution functional maps of orientation columns, "lighting up" in milliseconds with an SNR even better than that obtained with the slow intrinsic signals (see Fig. 2). Additional developments will undoubtedly introduce further improvement.

In summary, VSDI of cortical activity is a particularly attractive technique for providing new insights into the temporal aspects of mammalian brain function. Among its advantages over other methodologies are (1) direct recording of the summed membrane potential changes of neuronal populations, including fine dendritic and axonal processes; (2) ability to measure these repeatedly from the same cortical region over an extended period of time, using different experimental or stimulus conditions; (3) imaging spatiotemporal patterns of activity of neuronal populations with a submillisecond temporal resolution; and (4) selective visualization of neuronal assemblies (see below). Several related reviews have been published elsewhere (Tasaki and Warashina 1976; Waggoner and Grinvald 1977; Cohen et al. 1978; Waggoner 1979; Grinvald 1984, 1985; Cohen and Lesher 1986; De Weer and Salzberg 1986; Salzberg et al. 1986; Loew 1987; Orbach 1988; Grinvald et al. 1991; Kamino 1991; Cinelli and Kauer 1992; for more detailed reviews, see Grinvald et al. 1988, 1999; Grinvald and Hildesheim 2004; Grinvald and Petersen 2010).

DISTRIBUTED PROCESSING: THE SPREAD OF ACTIVITY FAR BEYOND THE RETINOTOPIC/SOMATOTOPIC REPRESENTATIONS

One outstanding question that has benefited from real-time optical imaging is that of the distance in the cortical surface across which activation by a sensory point stimulus spreads. As mentioned above, the voltage-sensitive dye signal in cortical tissue reflects, in the main, the postsynaptic potentials in the fine dendrites of cortical cells rather than action potentials in cell somata. VSDI is thus ideally suited to answer this question.

The frog retinotectal connections offer a system that is topographically well organized: Each spot of light on the retina activates a small region in the optic tectum. The first optical imaging study investigating the spread of activation concentrated on visualizing the topographic distribution of

sensory responses in the frog (Grinvald et al. 1984). The optical signals obtained from the tectum in response to discrete visual stimuli were found to correspond well to the known retinotopic map of the tectum. However, in addition to a focus of excitation, the spatial distribution of the signals showed smaller, delayed activity (3–20 msec) covering a much larger area than would be expected on the basis of classic single-unit mapping.

In rat primary somatosensory cortex, each whisker projects to a well-defined region termed the whisker barrel, and there is a simple somatotopic organization of the different whisker barrels side by side. This preparation thus offered a convenient opportunity to explore the question of activation spread in the mammalian brain. When the tip of a whisker was gently moved, optical signals were observed in the corresponding cortical barrel field (Derdikman et al. 2003). However, a discrepancy was noted between the size of an individual barrel, as recorded optically (1300 μm) and the histologically defined barrel (300–600 μm in layer 4 of the cortex, showing neuronal somata rather than processes). The reason for this difference is probably that most of the optical signal originates from the superficial cortical layers in which neurons extend long processes to neighboring barrels (Orbach et al. 1985; Kleinfeld and Delaney 1996; Takashima et al. 2001; Derdikman et al. 2003). Glutamate antagonists blocked the spread. Thus, postsynaptic activity in the dendritic processes could account for the detected spread (Petersen et al. 2003a,b). This lateral spread is both excitatory and inhibitory, and the balance probably depends on the stimulus parameters (Fig. 1C). Net surround inhibition was also documented at late times in the surround of an activated barrel (Orbach et al. 1985; Takashima et al. 2001; Derdikman et al. 2003).

In monkey striate cortex, retinotopic imaging experiments also showed activity over a cortical area much larger than predicted on the basis of standard retinotopic measurements in layer 4, but consistent with the anatomical finding of long-range horizontal connections in visual cortex (Gilbert and Wiesel 1983). The results of these experiments were used to calculate the cortical point spread function, which reflects the extent of cortical activation by retinal point stimuli. Figure 1 illustrates the cortical point spread function in macaque primary visual cortex. To show the relationship between the

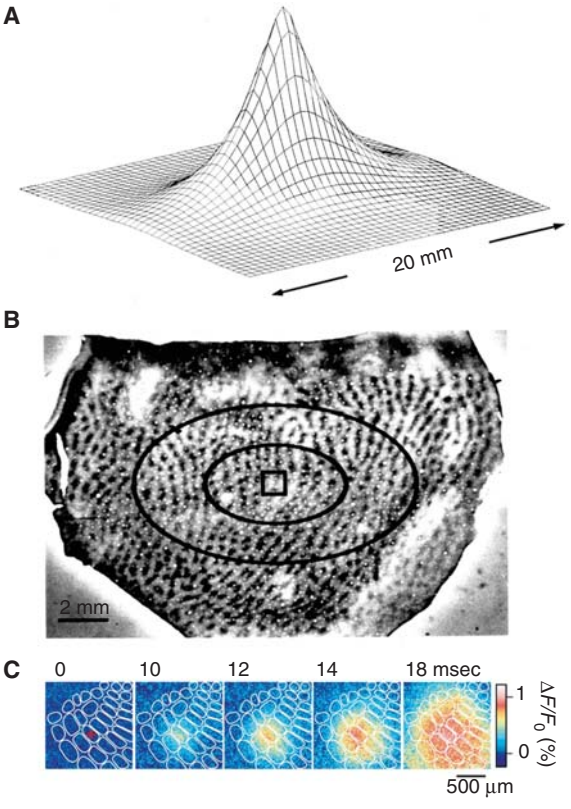

FIGURE 1. Many functional domains are activated during the processing of a small retinal image or a single whisker deflection. (*A*) Calculation of the activity spread from a small patch in layer 4 (a 1 × 1-mm square) within the upper cortical layers of a macaque. This cortical activation was produced by a retinal image of ~0.50° × 0.25° that was presented to both eyes. The space constants for the exponential activity spread measured with the dye experiments were 1.5 and 2.9 mm in the cortical axes perpendicular and parallel to the vertical meridian representation, respectively. (*B*) Direct activation in layer 4 (of the area within the square; calculated from retinotopic extracellular recordings) and the spread in layers 2/3 (elliptical contours; calculated from VSDI) are shown superimposed on a histological section showing the mosaics of cytochrome oxidase blobs, close to the border between cortical areas V1 and V2. The center ellipse shows the contour at which the amplitude of cortical activity drops to 37% of its peak. The larger ellipse shows the contour at which the spread amplitude drops to 14%. More than 10,000,000 neurons reside in the cortical area bounded by the large ellipse containing a regular mosaic of about 250 blobs. (*C*) The exact spatiotemporal pattern of the spread in the somatosensory cortex in response to a single barrel stimulation. The temporal resolution was 2 msec/frame. (*A*,*B*, Reprinted from Grinvald et al. 1994; *C*, data from Petersen et al. 2003a,b.)

observed spread and individual cortical modules, the spread function is projected on a histological section of cytochrome oxidase blobs (Fig. 1B). The stimulus used here caused spiking, activated only in neurons residing in the marked small square, which contains just four blobs. However, more than 200 blobs had access to the information carried by the signal spread, albeit at a lower amplitude. The apparent "space constant" for the spread was 1.5 mm along the cortical axis, parallel to the ocular dominance columns, and 3 mm along the perpendicular axis. The spread velocity was 0.1–0.2 m/sec (Grinvald et al. 1994). A recent study in anesthetized cats showed that this spreading subthreshold synaptic activity is priming the cortex and the cortex then responds differently to a subsequent stimulus; it has been reported that perception of motion when only stationary stimuli were displayed could be explained by this type of activity, which is totally elusive to unit recordings (Jancke et al. 2004).

The extensive lateral spread observed beyond the retinotopic borders in layer 4, both excitatory and inhibitory, indicates that the degree of distributed processing in primary visual cortex is much larger than often conceived—certainly a nontrivial challenge for theoreticians studying cortical networks. In these early studies of the visual response using VSDI, the spatial resolution did not enable exploration of such basic attributes of the visual response as orientation selectivity. Subsequent studies, described below, addressed this issue. Much higher spatial resolution data showing similar spread in the somatosensory cortex were first reported by Derdikman et al. (2003) and Petersen et al. (2003a) (Fig. 1C) and several subsequent papers from the same group (Petersen et al. 2004; Ferezou et al. 2006, 2007; Berger et al. 2007).

The sophisticated nature of the effect of the long-range spread as revealed in the visual cortex is discussed below.

LONG-RANGE HORIZONTAL SPREAD OF ORIENTATION SELECTIVITY IS CONTROLLED BY INTRACORTICAL COOPERATIVITY

During the last three decades, the intracortical anatomical connectivity made by the horizontal connections has been extensively explored in multiple species. It has generally been concluded that horizontal axons in visual cortex bind distant columns sharing a similar orientation preference. However, the functional selectivity of the horizontal spread has never been measured directly. One reason is that the connections made by the horizontal axons are difficult to record because they only have a subthreshold impact on their postsynaptic targets. Therefore, to unveil the functional expression of the horizontal connectivity, it is mandatory to have access to the activation of the horizontal network at the subthreshold, postsynaptic integration level. Chavane et al. (2011) reported a multiscale analysis of visually driven horizontal network activation, using direct population and intracellular measures of postsynaptic integration. VSDI shows that while global activation in response to a local stimulus shows long-range horizontal spread, the orientation-selective component of this response does not spread beyond the feedforward cortical imprint of the stimulus. Orientation selectivity decreases exponentially with horizontal distance. Therefore, beyond a distance of one hypercolumn, horizontal functional connectivity no longer obeys a binding rule preserving iso-orientation preference with this type of stimulus. Intracellular recordings show that this loss of orientation selectivity arises from the diversity of convergence patterns of intracortical synaptic input originating from beyond the classical receptive field.

In contrast, when increasing the spatial summation evoked by the stimulus—for example, by presenting annular stimuli—orientation-selective activation spreads beyond the feedforward imprint (compare Fig. 2A,B: the orientation map). It was therefore concluded that stimulus-induced cooperativity at the network level is needed for the emergence of long-range orientation-selective spread.

Chavane et al. (2011) shows two different dynamic behaviors of the same network for two distinct stimulus configurations: a single local stimulus does not propagate orientation preference through the long-range horizontal cortical connections, whereas stimulation imposing spatial summation and temporal coherence facilitates the build-up of propagating activity showing a strong orientation

 Cite this introduction as *Cold Spring Harb Protoc;* doi:10.1101/pdb.top089367

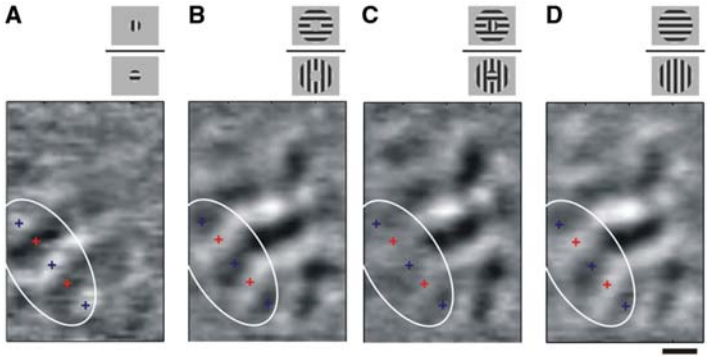

FIGURE 2. Horizontal spread and center-surround competition. (*A*) Area 18 differential map obtained by dividing the responses to horizontal versus vertical gratings presented through a central disk aperture (stimulus diameter 4° at an eccentricity of 7.6°; see cartoons). Orientation map is confined locally. (*B*) In comparison, displaying a larger grating through an annular aperture without stimulating the central disk (stimulus inner diameter, 4°; outer diameter, 12°; same eccentricity) results in the propagation of an orientation-selective signal within the cortical representation of the central disk region. (*C*) When both stimuli compete in a composite cross-oriented configuration, the orientation map disappears within the retinotopic representation of the central disk. (*D*) Control condition with iso-oriented center-surround configurations. The white contour encircles the expected retinotopic representation of the central disk. Scale bar, 1 mm.

preference. These observations do not necessarily contradict each other. They point to the possibility that complex stimulus configurations are allowed and expected based on activation within a locally confined region in visual space, whereas an iso-oriented stimulus with a large spatial extent supports the expectation of that specific orientation throughout a yet-larger area.

DYNAMICS OF SHAPE PROCESSING AT SUBCOLUMNAR RESOLUTION

A key goal for functional brain mapping is to obtain single-condition maps: that is, to acquire the pattern of activation evoked by a single stimulus condition, without the need to perform differential imaging of two orthogonal stimuli. This is important because for resolving most of the questions requiring imaging, truly orthogonal stimuli cannot be defined, and because analyzing single-condition data reveals processes that are difficult or impossible to see with differential data. With the technical advances in VSDI, we were able to obtain time series of single-condition maps millisecond by millisecond, at subcolumnar resolution. We used it to revisit fundamental questions regarding the emergence of orientation selectivity in visual cortex (Sharon and Grinvald 2002).

Two families of mechanisms have been proposed to play a role in the emergence of the highly orientation-selective responses of cortical visual neurons, a property not shared by their thalamic inputs. Feedforward-only models suggest appropriate alignment of thalamic input as the mechanism, whereas recurrent models suggest that intracortical interactions are more important. Measuring the dynamics of the response to the input by visual cortex, as enabled by VSDI, is relevant to this question because the feedforward explanation predicts that orientation selectivity should remain constant with time from stimulus onset, whereas if recurrent interactions are important, then selectivity should change as the cortical network performs its processing.

To answer the question of dynamics of orientation selectivity, we first acquire the crucial high-quality single-condition maps. A time series of the initial response is shown in Figure 3A for two orthogonal orientations. As soon as the response is observable, the two orthogonal stimuli are shown to preferentially activate complementary patches of cortex. This pattern is, of course, easily observed in the differential map (Fig. 3B,C). To calculate orientation tuning curves, however, differential maps and time courses are of no use, and single-condition responses are needed (Fig. 3D).

In experiments in which six different orientations were shown, the tuning curves at each point in time could be calculated directly from the single-condition responses (Fig. 3E). The immediate

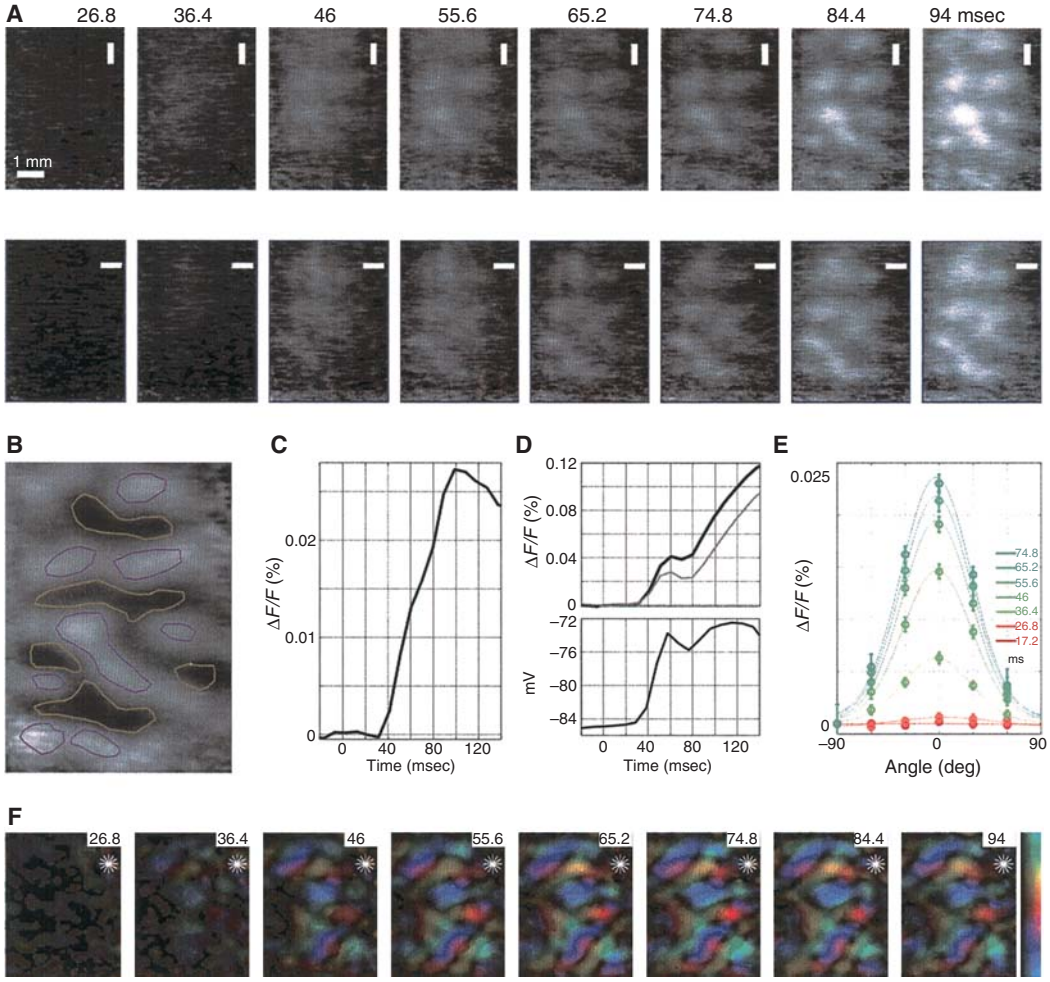

FIGURE 3. The dynamics of orientation tuning. (*A*) The two rows show the time series of single-condition orientation maps, in response to two orthogonal stimuli. (*B*) Spatial pattern revealed by differential imaging. (*C*) Temporal pattern of differential activity. The deceleration–acceleration (DA) notch is hardly visible here, thus it was overlooked in earlier studies. (*D*) (*Top*) The time course of the evoked response to preferred (black) and orthogonal (gray) orientations, calculated from the time series of single-condition maps shown in (*A*). The two responses have the same onset latency (~30 msec); the response to the preferred orientation is larger from the onset. The striking feature of the evoked responses is the DA notch. (*C* and *D*) were calculated for pixels in the regions marked in *B*. (*Bottom*) Confirmation of the DA notch with intracellular recordings performed in our laboratory (Sterkin et al. 1998). The notch in the intracellular data appears at the same time as that in the dye data, at ~50–80 msec. After the notch, the dye response continues to grow a lot more than the intracellular response; this could be attributable to the fact that the dye measures membrane potential changes over the entire dendritic arborization, and not just in the soma. (*E*) Orientation tuning curves at different times after stimulus onset, from another experiment. The curves after response onset (green) have the same shape but different amplitudes. The baseline of the curves was shifted to facilitate comparison. (*F*) Time series of orientation preference maps in polar depiction: Color represents preferred orientation (top to bottom of color scale on right is 0°–180°), and brightness represents amplitude of differential response (*left* to *right* of color scale is 0%–0.05%). Preferred orientation is steady from response onset. The VSDI data in *A*–*D* are raw, unfiltered. (Modified from Sharon and Grinvald 2002.)

impression is that of tuning curves with a constant shape but changing amplitude. Indeed, the half-width at half-height of tuning curves were steady right from response onset (Sharon and Grinvald 2002). Sustained intracortical processing, therefore, does not seem to be needed to determine orientation tuning width, at least for the majority of the population.

There are additional aspects of the response that affect orientation selectivity, not just tuning width. As shown in Figure 3C, the modulation depth of the response (difference between preferred and orthogonal) does change, decreasing after a peak at 100 msec. An intriguing phenomenon is

Cite this introduction as *Cold Spring Harb Protoc*; doi:10.1101/pdb.top089367

nearly undetectable in the differential time course, but very obvious when considering the evoked single-condition responses (Fig. 3D). There is a notch in the evoked response, equivalent to a deceleration followed by acceleration in the rise time—this is termed the evoked DA (deceleration–acceleration) notch. It is likely caused by a suppressive mechanism peaking at 50–80 msec. These are the kind of dynamics that one would expect from intracortical processing. Furthermore, the evoked DA notch is more pronounced in response to the orthogonal stimulus than to the preferred stimulus (see Fig. 3D; Sharon and Grinvald 2002).

These results suggest that thalamic input may be the major determinant of orientation tuning width for most cortical neurons, but that intracortical processing is critical in amplifying the orientation-selective component of the response. They also hint that intracortical suppression contributes to this process by preventing the orthogonal response from increasing as rapidly as the response to the preferred orientation.

SELECTIVE VISUALIZATION OF NEURONAL ASSEMBLIES

It has been suggested that neurons operate in assemblies (Hebb 1949), networks of neurons that may or may not reside locally, and which communicate coherently to perform the computations required for various tasks. Thus, in VSDI, neurons at the recorded site may belong to different neuronal assemblies. To explore cortical computations, it is often interesting to look at the dynamics of individual neuronal assemblies, rather than at the activity originating from heterogeneous populations containing many assemblies. A significant contribution of real-time optical imaging has been the visualization of the dynamics of coherent neuronal assemblies (i.e., neuronal assemblies in which the activity of cells is time-locked). The firing of a single neuron is used as a time reference to selectively visualize activity that is synchronized with it (i.e., only the activity in the assembly to which the reference neuron belongs [Grinvald et al. 1989, 1991; Arieli et al. 1995]).

To isolate and study the spatiotemporal organization of neuronal assemblies, VSDI was combined with single-unit recordings and subsequent spike-triggered averaging of the optical recordings. With sufficient averaging (Fig. 4), the neuronal activity not time locked to the reference neuron was averaged out, enabling the selective visualization of those cortical locations in which activity consistently occurred coherently with the firing of the reference neuron. The visual cortex (area 18) of anesthetized cats was stained with the dye RH-795, and either ongoing (spontaneous, in the absence of visual stimulation) or evoked activity was recorded continuously for 70 sec. We simultaneously recorded optical signals from 124 sites, together with electrical recordings of LFP and single unit recordings (one to three isolated units recorded with the same electrode). The spike-triggered averaging analysis showed that the averaged optical signal at the electrode site had a peak that temporally coincided with the occurrence of a peak in the LFP. The dye signal was similar to the LFP recorded from the same site. This indicates the expected result that many neurons next to the electrode site had coherent firing patterns. Interestingly, however, the dye signals more distant from the electrophysiological recording site were heterogeneous, indicating that VSDI provides a better spatial resolution than field potential recordings.

In 88% of the neurons recorded during spontaneous activity, a significant correlation was found between the occurrence of a spike and the optical signal recorded in a large cortical region surrounding the recording site, including cortical sites up to 6 mm away. This result indicates that spontaneous activity of single neurons is not an independent process but is time-locked to the firing or the synaptic inputs from numerous neurons, all activated in a coherent fashion, even without a sensory input. Surprisingly, it was found that the amplitude of this coherent ongoing activity, recorded optically, was often almost as large as the activity evoked by optimal visual stimulation. The amplitude of the ongoing activity, which was directly and reproducibly related to the spontaneous spikes of a single neuron, was, on average, as high as 54% of the amplitude of the visually evoked response by optimal sensory stimulation, recorded optically. Coherent activity was detected even at distant cortical sites up to 6 mm apart. On the other hand, in a few cases, it was found that the spontaneous activity of two

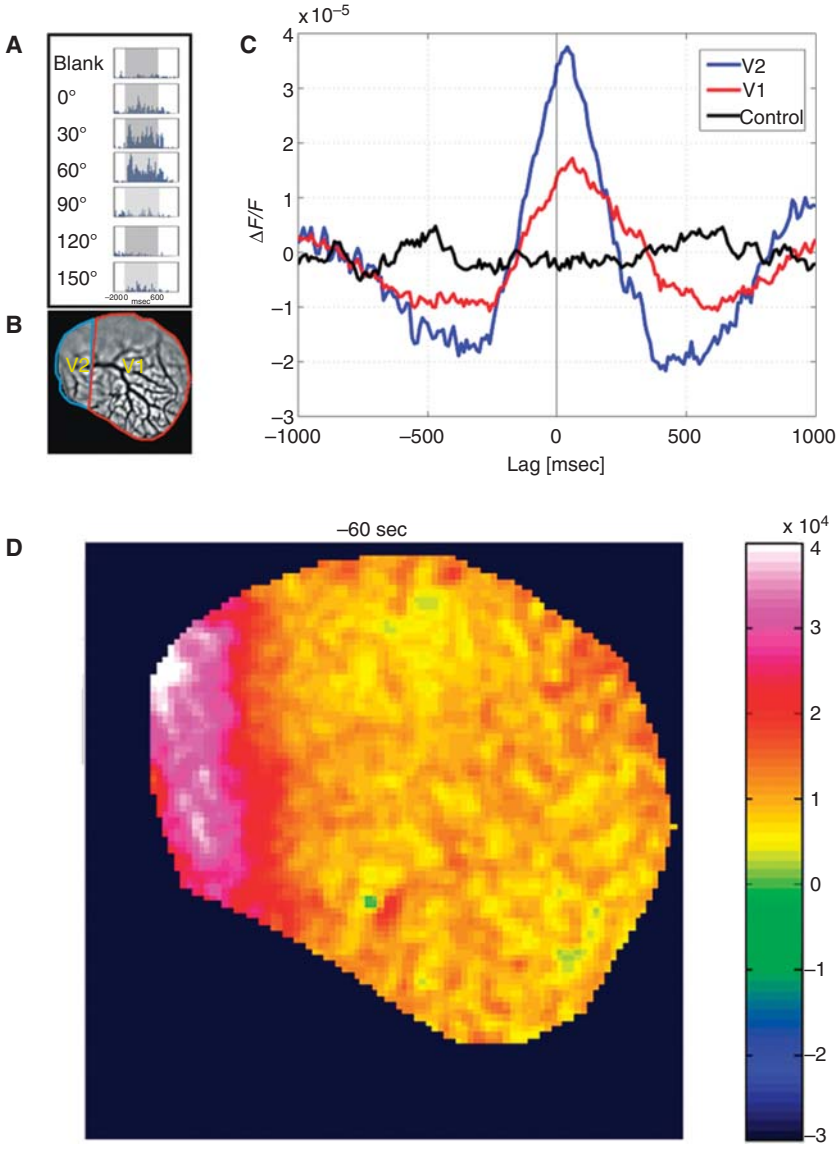

FIGURE 4. Visualization of coherent neuronal assemblies across visual areas. (*A*) The tuning properties of a single cell in V1 of primary visual cortex of the awake monkey, which was used for the spike-triggered averaging. (*B*) Cartoon of the imaged area showing the V1/V2 border that was identified by mapping the ocular dominance columns in V1. (*C*) The time course of spike-triggered average (STA) of the optical signal from V2 (blue curve) as well as the optical signal from V1 (red curve) on the time of the firing of the V1 reference neuron. Evidently, whenever this cell fired, there was activity over a large area in V1 as well as V2. In fact, in this case, whenever this cell in V1 fired there was larger coherent activity in V2 than in V1. (*D*) The average spatial pattern 60 msec before the V1 action potential occurred is shown. (Courtesy of David Omer and Amiram Grinvald; unpublished results.)

adjacent neurons, isolated by the same electrode and sharing the same orientation preference, was correlated with two different spatiotemporal patterns of coherent activity, suggesting that adjacent neurons in the same orientation column can belong to different neuronal assemblies.

A subsequent study explored the relationship between the spatial pattern of population activity coherent with a single neuron's spikes during spontaneous and evoked activity. They were found to be very similar. Furthermore, it has been reported that the firing rate of a spontaneously active single neuron strongly depends on the instantaneous spatial pattern of ongoing population activity in a large cortical area: During spontaneous activity, whenever the instantaneous spatial population pattern correlated highly with the spatial population pattern evoked by the preferred stimulus of the recorded

Cite this introduction as *Cold Spring Harb Protoc*; doi:10.1101/pdb.top089367

neuron, its firing rate increased. This was used to reconstruct the spontaneous activity of single neurons based on the global spontaneous activity (Tsodyks et al. 1999).

These results indicate that the spontaneous firing of single neurons is tightly linked to the cortical networks in which they are embedded. The idea of a neural network is a central concept in theoretical brain research, and it is finally possible to directly visualize the cortical networks and their states in action, at high spatiotemporal resolution. Exploring cortical states is likely to reveal new fundamental principles about neural strategies for cortical processing, representations of objects, memories, context, expectations, and particularly about the interplay between internal cortical representations and the sensory input in primary sensory areas.

The finding that the amplitude of spontaneous ongoing activity in neuronal assemblies is nearly as large as evoked activity suggests that it may play an important role in shaping spatiotemporal patterns evoked by sensory stimuli (Arieli et al. 1996a). Therefore, it is important to be able to study the dynamics of ongoing and evoked activity without signal averaging.

ONGOING ACTIVITY IN CORTICAL PROCESSING: IMAGING WITHOUT SIGNAL AVERAGING

Despite the large biological noise originating from respiration and heartbeat pulsations, reliable VSDI was accomplished even without signal averaging, using offline correction procedures instead. This allowed, for the first time, exploration of the dynamics of spontaneous ongoing population activity and its interaction with evoked activity.

In the mammalian visual cortex, evoked responses to repeated presentations of the same stimulus show a large variability. It has been found that this variability results from ongoing activity, reflecting the dynamic state of the cortical network. The central finding in the initial studies of ongoing activity using VSDI without signal averaging was that, despite this large variability, the evoked responses in single trials can be predicted by taking into account the preceding ongoing activity.

The evoked response in a given single-stimulus presentation can be predicted by summing the preceding ongoing activity with the evoked response, averaged over many presentations. This prediction is valid as long as the ongoing activity pattern, which presumably continues to change during the evoked response, is still similar to the initial state (Arieli et al. 1996a).

These findings indicate that the old notions of what "noise" in brain activity represents may have to be revised. Because the ongoing activity is often very large, it would be expected to play a major role in cortical function. It may provide the neuronal substrate for the dependence of sensory information processing on context, attention, behavioral and consciousness states, memory retrieval, and other aspects of cognitive function. Preliminary experiments have shown that behavior itself is also affected by ongoing activity (Arieli et al. 1996b).

The newly improved SNR of VSDI enabled exploration of the dynamics of ongoing activity and its relation to internal representations of sensory attributes. It was found that ongoing activity in the visual cortex of the anesthetized cat is composed of dynamically switching intrinsic cortical states, many of which closely correspond to orientation maps. When such an orientation state emerged spontaneously, it spanned several cortical hypercolumns and was usually followed by a state corresponding to a proximal orientation. Otherwise, it dissolved into an unrecognized state or noisy pattern after a few tens of milliseconds (Grinvald et al. 1991; Shoham et al. 1991; Kenet et al. 1997, 2003).

The above findings raised the hypothesis that dynamically switching cortical states could express the brain's internal context, representing and influencing memory, perception, and behavior. Such studies obviously require the use of the awake behaving monkey rather than anesthetized subjects. This is indeed being explored in behaving monkeys as described by Slovin et al. (2002) and by Omer and Grinvald as described in Grinvald and Petersen (2010). They performed VSDI of ongoing cortical activity in the visual cortices of awake monkeys simultaneously with measurements of single-unit activity and the local-field potential. They found coherent activity also in the awake monkey. Figure 4 shows the tuning properties of the reference cell (Fig. 4A), the border between the two imaged areas

V1 and V2 (Fig. 4B), time course of the coherent activity in area V1 (red) and V2 (blue; Fig. 4C), and the instantaneous spatial pattern of the assembly activity just before the action potential of the reference neuron (Fig. 4D). Overall, the dynamics were very different from that found in anesthetized cats and in a single epoch, it was not possible to recognize any pattern that looked like the known functional architecture. Nevertheless, it was found that such patterns do appear: The pairwise correlation among pixels of known functional architecture as a function of the orientation difference between these pixels or their ocularity index had the same stereotypic shape for evoked activity and for spontaneous epochs. Similar results were also obtained in the anesthetized monkeys. However, in the anesthetized monkeys spontaneous cortical activity that resembled the functional architecture was also found just like in the anesthetized cats (Muir et al. 2011). These results underscore the importance of carrying out experiments on awake behaving animals because the spatiotemporal patterns of activity are so drastically different.

LONG-TERM VSDI OF CORTICAL DYNAMICS IN BEHAVING MONKEYS

Chronic optical imaging based on newer voltage-sensitive dyes was developed to facilitate exploration of the spatial and temporal patterns underlying higher cognitive functions in the neocortex of behaving monkeys. The technique was used to explore cortical dynamics, with high spatial and temporal resolution, over periods of up to 1 yr from the same patch of cortex (Slovin et al. 2002). The visual cortices of trained macaques were stained one to three times a week and, immediately after each staining session, the monkey started to perform a simple behavioral task, while the primary visual cortex (V1) and the secondary area (V2) were imaged with a fast optical imaging system. Long-term, repeated VSDI from the same cortical area did not disrupt the normal cortical architecture, as confirmed repeatedly by optical imaging based on intrinsic signals. The spatial patterns of functional maps obtained by VSDI in response to full-field stimuli were essentially identical to those obtained from the same patch of cortex by imaging based on intrinsic signals. On comparing the relative amplitudes of the evoked signals and differential maps obtained using these two different imaging methods, it was found that the relative contribution of subthreshold versus spiking activity was higher in the voltage-sensitive dye signal than in the intrinsic signal. In the awake monkey, evoked activity could also be detected without signal averaging, similarly to the above-mentioned anesthetized cat experiments.

The same approach also proved useful in the exploration of the motor cortex. Electrical recording studies during Go/No-Go tasks found that primary motor cortex (M1) neurons display changes in activity which begins primarily after a Move cue, whereas dorsal premotor (PMd) neurons, known to be engaged in motor planning, display changes in activity that can begin during the Instructed Delay periods. One monkey was trained to perform a Go/No-Go task. The monkey began a trial by placing his hand over a small photodiode in front of him. This caused a small white square to appear on a computer screen. After a variable precue period (3000–4000 msec), the white square was changed to red (Go mode) or green (No-Go mode). Then, after a variable Instructed Delay period (300–1500 msec), a luminance change of the square told the monkey to follow the prior instruction: Uncover (Go) or continue to cover the photodiode (No-Go). In the PMd, the VSD signal changes began shortly after the onset of the Go or No-Go instructions (i.e., at the start of the Instructed Delay periods). Relatively large signals were observed in the PMd area during both Go and No-Go. The VSD signals were much smaller in M1 during the No-Go mode. These observations suggest that the preparation to perform or withhold a motor response is associated mainly with marked subthreshold activity in the PMd (Strick et al. 2003).

This work shows a new way of recording and analyzing the dynamics of population activity in behaving monkeys, with high spatial and temporal resolution. The combination of VSDI with traditional electrical recordings can also be readily adapted to facilitate the selective visualization of coherent activity in neuronal assemblies involved in dynamic representations and processing of sensory input, as well as in the planning, control, and execution of motor output (Slovin et al. 2003; Strick et al. 2003). Another powerful combination is described below.

 Cite this introduction as *Cold Spring Harb Protoc;* doi:10.1101/pdb.top089367

COMBINED VSDI AND MICROSTIMULATION IN FRONTAL AND MOTOR CORTEX

Despite extensive use of microstimulation in various brain regions to affect neuronal and behavioral responses (see, e.g., Newsome et al. 1989; Cohen and Newsome 2004), the spatiotemporal pattern of activation it evokes has not been characterized, leaving open many questions about the spread of activation, both direct, from the electric shock itself, and indirect, from synaptic activity. Microstimulation can be incorporated into VSDI studies of the frontal and motor cortex of awake monkeys.

The frontal eye field and neighboring area, 8Ar, of the primate cortex are involved in programming and execution of saccades. Electrical microstimulation in these regions elicits short-latency contralateral saccades. To determine how spatiotemporal dynamics of microstimulation-evoked activity are converted into saccade plans, the combination of VSDI and microstimulation in behaving monkeys was used. Short stimulation trains evoked a rapid and widespread wave of depolarization followed by an unexpectedly large and prolonged hyperpolarization. During this hyperpolarization, saccades are almost exclusively ipsilateral, suggesting an important role for hyperpolarization in determining saccade goal (Seidemann et al. 2002). This result shows that neural activity, with composite spatiotemporal dynamics, can be elicited by microstimulation and emphasizes the importance of further characterization of microstimulation-evoked activity for the interpretation of the behavioral effects of microstimulation.

Intracortical stimulation has also been used as a tool to discover the pattern of muscle and/or movement representation in motor areas of the cortex. VSDI was used to examine the patterns of activation evoked by different stimulation parameters in the primary motor cortex (M1). Those experiments used much finer stimulation conditions than the previous work. Single cathodal pulses in M1 (15–30 μA, 0.2-msec duration) evoked short-latency dye responses that continued for 40–50 msec after the onset of stimulation. These responses spread in an asymmetric manner from the stimulation site in M1; the width of the activated area was ~1.5–3 mm. Single pulses, >15 μA, also evoked activity at spatially separate sites within M1. Short trains of pulses in M1 (2–20 pulses, 330–500 Hz, and 30–100 μA) produced activation that spread from the electrode site to adjacent premotor areas and to the contralateral hemisphere. A distinct hyperpolarization followed the activation produced by a high-current (>60 μA), short-stimulus train (2–20 pulses). Finally, long-stimulus trains (70 μA, 200 pulses, and 330 Hz) evoked activation that spread over large portions of M1 and the adjacent premotor areas. The responses outlasted the stimulus train by several hundred milliseconds (Slovin et al. 2003). These results emphasize the importance of considering the spread of activation when evaluating the results of M1 stimulation.

CONCLUSIONS AND OUTLOOK

VSDI is based on the use of voltage-sensitive dyes, and the quality of results it produces is therefore limited by the properties of these dyes. The results presented here indicate that the technique has finally matured sufficiently to explore the neocortex in ways never feasible before. Furthermore, it is expected that the development of new voltage-sensitive dyes and future genetic engineering of suitable in vivo probes (see, e.g., Miyawaki et al. 1997; Siegel and Isacoff 1997) will make the experiments much easier and will substantially improve the quality of the results. Of particular importance are probes that will stain only specific cell types and/or specific cellular compartments (e.g., axons, somata, and dendrites). Additional developments of other technologies, using second-harmonic generation (Millard et al. 2003) and multiphoton and three-dimensional imaging, are highly desirable. Similarly, excitation at the red edge of existing VSDs has been shown to provide up to 10-fold larger fractional change in the VSD signal size (Kuhn and Fromherz 2003; Kuhn et al. 2004). Because VSDI excels at revealing spatiotemporal patterns of the synaptic potential—the input to a neocortical region, but lacking sensitivity to spiking its output—it should be highly fruitful to combine it with the new approach to calcium imaging in vivo that primarily reflects the output (Stosiek et al. 2003). To increase

the dimensionality of meaningful neurophysiological data obtained from the same patch of cortex, VSDI should be combined with targeted tracer injections, retrograde labeling, microstimulation, and intracellular and extracellular recordings. VSDI, combined with electrical recordings, allows investigators to obtain information about neuronal activity in coherent neuronal assemblies, within the neocortex, at subcolumnar resolution.

Although there is fast progress in the development of imaging techniques, to date no alternative imaging technique for visualizing functional organization in the living brain provides a comparable spatial and temporal resolution. It is this level of resolution that makes it possible to address questions of both *where* and *when* processing is performed, promising that this technique will contribute to the study of *how*—revealing fundamental principles of neural coding and processing strategies at the population level.

ACKNOWLEDGMENTS

We thank Yuval Toledo and Alexander Sterkin for their dedicated programming assistance, and our previous coworkers, Ron Frostig, Edmund Lieke, Doron Shoham, Daniel Glaser, Amos Arieli, Eyal Seidemann, Tal Kenet, Misha Tsodyks, Dirk Jancke, and Frederick Chavane, for their original contributions. This work was supported by grants from the Grodetsky Center, Goldsmith, Glasberg, Heineman, and Korber foundations, Ministry of Science (MOS) and Bundesministerium für Bildung, Forschung und Technologie (BMBF), the Israeli Science Foundation, and the European Commission Project 15803, Daisy.

REFERENCES

Arieli A, Grinvald A. 2002. Combined optical imaging and targeted electrophysiological manipulations in anesthetized and behaving animals. *J Neurosci Methods* **116:** 15–28.

Arieli A, Shoham D, Hildesheim R, Grinvald A. 1995. Coherent spatiotemporal pattern of ongoing activity revealed by real time optical imaging coupled with single unit recording in the cat visual cortex. *J Neurophysiol* **73:** 2072–2093.

Arieli A, Sterkin A, Grinvald A, Aertsen A. 1996a. Dynamics of ongoing activity: Explanation of the large variability in evoked cortical responses. *Science* **273:** 1868–1871.

Arieli A, Donchin O, Aertsen A, Bergman H, Gribova A, Grinvald A, Vaadia E. 1996b. The impact of ongoing cortical activity on evoked potential and behavioral responses in the awake behaving monkey. *Neuroscience* **22:** 2022. (Abstr.)

Arieli A, Grinvald A, Slovin H. 2002. Dural substitute for long-term imaging of cortical activity in behaving monkeys and its clinical implications. *J Neurosci Methods* **114:** 119–133.

Berger T, Borgdorff AJ, Crochet S, Neubauer FB, Lefort S, Fauvet B, Ferezou I, Carleton A, Luscher HR, Petersen CCH. 2007. Combined voltage and calcium epifluorescence imaging in vitro and in vivo reveals subthreshold and suprathreshold dynamics of mouse barrel cortex. *J Neurophysiol* **97:** 3751–3762.

Chavane F, Sharon D, Jancke D, Marre O, Frégnac Y, Grinvald A. 2011. Lateral spread of orientation selectivity in V1 is controlled by intracortical cooperativity. *Front Syst Neurosci* **5:** 4.

Cinelli AR, Kauer JS. 1992. Voltage sensitive dyes and functional-activity in the olfactory pathway. *Annu Rev Neurosci* **15:** 321–352.

Cinelli AR, Kauer JS. 1995. Salamander olfactory-bulb neuronal-activity observed by video-rate, voltage sensitive dyes imaging. 2. Spatial and temporal properties of responses evoked by electric stimulation. *J Physiol* **73:** 2033–2052.

Cinelli AR, Neff SR, Kauer JS. 1995. Salamander olfactory bulb neuronal activity observed by video rate, voltage-sensitive dye imaging. I. Characterization of the recording system. *J Neurophysiol* **73:** 2017–2032.

Cohen LB, Lesher S. 1986. Optical monitoring of membrane potential: Methods of multisite optical measurement. *Soc Gen Physiol Ser* **40:** 71–99.

Cohen MR, Newsome WT. 2004. What electrical microstimulation has revealed about the neural basis of cognition. *Curr Opin Neurobiol* **14:** 169–177.

Cohen LB, Salzberg BM, Davila HV, Ross WN, Landowne D, Waggoner AS, Wang CH. 1974. Changes in axon fluorescence during activity: Molecular probes of membrane potential. *J Membr Biol* **19:** 1–36.

Cohen LB, Slazberg BM, Grinvald A. 1978. Optical methods for monitoring neurons activity. *Annu Rev Neurosci* **1:** 171–182.

Derdikman D, Hildesheim R, Ahissar E, Arieli A, Grinvald A. 2003. Imaging spatio-temporal dynamics of surround inhibition in the barrels somatosensory cortex. *J Neurosci* **23:** 3100–3105.

De Weer P, Salzberg BM, eds. 1986. *Optical methods in cell physiology*. Society of General Physiologists Series, Vol. 40. Society of General Physiologists and Wiley-Interscience, New York.

Ferezou I, Bolea S, Petersen CC. 2006. Visualizing the cortical representation of whisker touch: Voltage-sensitive dye imaging in freely moving mice. *Neuron* **50:** 617–629.

Ferezou I, Haiss F, Gentet LJ, Aronoff R, Weber B, Petersen CC. 2007. Spatiotemporal dynamics of cortical sensorimotor integration in behaving mice. *Neuron* **56:** 907–923.

Gilbert CD, Wiesel TN. 1983. Clustered intrinsic connections in cat visual cortex. *J Neurosci* **3:** 1116–1133.

Grinvald A. 1984. Real time optical imaging of neuronal activity: From single growth cones to the intact brain. *Trends Neurosci* **7:** 143–150.

Grinvald A, Hildesheim R. 2004. VSDI: A new era in functional imaging of cortical dynamics. *Nat Rev Neurosci* **5:** 874–885.

Grinvald A, Petersen CCH. 2010. Imaging the dynamics of neocortical population activity in behaving and freely moving mammals. In *Membrane potential imaging in the nervous system: Methods and applications* (ed. Zecevic D, Canepari M), pp. 113–124. Springer Science+Business Media, New York.

Grinvald A, Salzberg BM, Cohen LB. 1977. Simultaneous recordings from several neurons in an invertebrate central nervous system. *Nature* **268:** 140–142.

Grinvald A, Cohen LB, Lesher S, Boyle MB. 1981. Simultaneous optical monitoring of activity of many neurons in invertebrate ganglia, using a 124 element "Photodiode" array. *J Neurophysiol* **45:** 829–840.

Grinvald A, Manker A, Segal M. 1982a. Visualization of the spread of electrical activity in rat hippocampal slices by voltage sensitive optical probes. *J Physiol* **333:** 269–291.

Grinvald A, Hildesheim R, Farber IC, Anglister L. 1982b. Improved fluorescent probes for the measurement of rapid changes in membrane potential. *Biophys J* **39:** 301–308.

Grinvald A, Anglister L, Freeman JA, Hildesheim R, Manker A. 1984. Real time optical imaging of naturally evoked electrical activity in the intact frog brain. *Nature* **308:** 848–850.

Grinvald A, Anglister L, Freeman JA, Hildesheim R, Manker A. 1985. Real-time optical mapping of neuronal activity: From single growth cones to the intact mammalian brain. *Annu Rev Neurosci* **8:** 263–305.

Grinvald A, Lieke E, Frostig RD, Gilbert CD, Wiesel TN. 1986. Functional architecture of cortex revealed by optical imaging of intrinsic signals. *Nature* **324:** 361–364.

Grinvald A, Frostig RD, Lieke E, Hildesheim R. 1988. Optical imaging of neuronal activity. *Physiol Rev* **68:** 1285–1366.

Grinvald A, Frostig RD, Ts'o DY, Lieke E, Arieli A, Hildesheim R. 1989. Optical imaging of activity in the visual cortex. In *Neuronal mechanisms of visual perception* (ed. Lam D, Gilbert CD), pp. 117–136. Portfolio Press, Woodlands, TX.

Grinvald A, Bonhoeffer T, Malonek D, Shoham D, Bartfeld E, Arieli A, Hildesheim R, Ratzlaff E. 1991. Optical imaging of architecture and function in the living brain. In *Memory: Organization and locus of change* (ed. Squire L), pp. 49–85. Oxford University Press, New York.

Grinvald A, Lieke EE, Frostig RD, Hildesheim R. 1994. Cortical point-spread function and long-range lateral interactions revealed by real-time optical imaging of macaque monkey primary visual cortex. *J Neurosci* **14:** 2545–2568.

Grinvald A, Shoham D, Shmuel A, Glaser ED, Vanzetta I, Shtoyerman E, Slovin H, Wijnbergen C, Hildesheim R, Sterkin A, et al. 1999. In-vivo optical imaging of cortical architecture and dynamics. In *Modern techniques in neuroscience research* (ed. Windhorst U, Johansson H), pp. 893–969. Springer, New York.

Hebb DO. 1949. The first stage of perception: Growth of the assembly. In *The organization of behavior: A neuropsychological theory*, pp. 60–78. Wiley, New York.

Hirota A, Sato K, Momosesato Y, Sakai T, Kamino K. 1995. A new simultaneous 1020 site optical recording system for monitoring neuronal activity using voltage sensitive dyes. *J Neurosci Methods* **56:** 187–194.

Hubel DH, Wiesel TN. 1962. Receptive fields, binocular interactions and functional architecture in the cat's visual cortex. *J Physiol* **160:** 106–154.

Iijima T, Matosomoto G, Kisokoro Y. 1992. Synaptic activation of rat adrenal-medula examined with a large photodiode array in combination with voltage sensitive dyes. *Neuroscience* **51:** 211–219.

Jancke D, Chavane F, Naaman S, Grinvald A. 2004. Imaging cortical correlates of a visual illusion. *Nature* **428:** 424–427.

Kamino K. 1991. Optical approaches to ontogeny of electrical activity and related functional-organization during early heart development. *Physiol Rev* **71:** 53–91.

Kauer JS. 1988. Real-time imaging of evoked activity in local circuits of the salamander olfactory bulb. *Nature* **331:** 166–168.

Kauer JS, Senseman DM, Cohen MA. 1987. Odor-elicited activity monitored simultaneously from 124 regions of the salamander olfactory bulb using a voltage-sensitive dye. *Brain Res* **25:** 255–261.

Kenet T, Arieli A, Grinvald A, Tsodyks M. 1997. Cortical population activity predicts both spontaneous and evoked single neuron firing rates. *Neurosci Lett* **48:** S27.

Kenet T, Grinvald A, Tsodyks M, Arieli A. 2003. Spontaneously occurring cortical representations of visual attributes. *Nature* **425:** 954–956.

Kleinfeld D, Delaney KR. 1996. Distributed representation of vibrissa movement in the upper layers of somatosensory cortex revealed with voltage-sensitive dyes. *J Comp Neurol* **375:** 89–108.

Konnerth A, Orkand RK. 1986. Voltage sensitive dyes measure potential changes in axons and glia of frog optic nerve. *Neurosci Lett* **66:** 49–54.

Kuhn B, Fromherz P. 2003. Anellated hemicyanine dyes in neuron membrane: Molecular stark effect and optical voltage recording. *J Phys Chem B* **107:** 7903–7913.

Kuhn B, Fromherz P, Denk W. 2004. High sensitivity of stark-shift voltage-sensing dyes by one- or two-photon excitation near the red spectral edge. *Biophys J* **87:** 631–639.

Lev-Ram R, Grinvald A. 1986. K^+ and Ca^{2+} dependent communication between myelinated axons and oligodendrocytes revealed by voltage-sensitive dyes. *Proc Natl Acad Sci* **83:** 6651–6655.

Loew LM. 1987. *Optical measurement of electrical activity*. CRC Press, Boca Raton, FL.

Millard AC, Jin L, Lewis A, Loew LM. 2003. Direct measurement of the voltage sensitivity of second-harmonic generation from a membrane dye in patch-clamped cells. *Optics Lett* **28:** 1221–1223.

Miyawaki A, Llopis J, Heim R, Caffery JM, Adams JA, Ikura M, Tsien RY. 1997. Fluorescent indicators for Ca^{2+} based on green fluorescent proteins and calmodulin. *Nature* **388:** 882–887.

Mountcastle VB. 1957. Modality and topographic properties of single neurons of cat's somatic sensory cortex. *J Neurophysiol* **20:** 408–434.

Muir DR, Da Costa NM, Girardin CC, Naaman S, Omer DB, Ruesch E, Grinvald A, Douglas RJ. 2011. Embedding of cortical representations by the superficial patch system. *Cereb Cortex* **21:** 2244–2260.

Newsome WT, Britten KH, Movshon JA. 1989. Neuronal correlates of a perceptual decision. *Nature* **341:** 52–54.

Orbach HS. 1988. Monitoring electrical activity in rat cerebral cortex. In *Spectroscopic membrane probes* (ed. Loew LM), Vol. 3, pp. 115–135. CRC Press, Boca Raton, FL.

Orbach HS, Cohen LB. 1983. Simultaneous optical monitoring of activity from many areas of the salamander olfactory bulb. A new method for studying functional organization in the vertebrate CNS. *J Neurosci* **3:** 2251–2262.

Orbach HS, Cohen LB, Grinvald A. 1985. Optical mapping of electrical activity in rat somatosensory and visual cortex. *J Neurosci* **5:** 1886–1895.

Petersen CCH, Grinvald A, Sakmann B. 2003a. Spatiotemporal dynamics of sensory responses in layer 2/3 of rat barrel cortex measured in vivo by voltage-sensitive dye imaging combined with whole-cell voltage recordings and anatomical reconstructions. *J Neurosci* **23:** 1298–1309.

Petersen CCH, Hahn T, Mehta M, Grinvald A, Sakmann B. 2003b. Interaction of sensory responses with spontaneous depolarization in layer 2/3 barrel cortex. *Proc Natl Acad Sci* **100:** 13638–13643.

Petersen CCH, Brecht M, Hahn TT, Sakmann B. 2004. Synaptic changes in layer 2/3 underlying map plasticity of developing barrel cortex. *Science* **304:** 739–742.

Ross WN, Reichardt LF. 1979. Species-specific effects on the optical signals of voltage sensitive dyes. *J Membr Biol* **48:** 343–356.

Salzberg BM, Davila HV, Cohen LB. 1973. Optical recording of impulses in individual neurons of an invertebrate central nervous system. *Nature* **246:** 508–509.

Salzberg BM, Grinvald A, Cohen LB, Davila HV, Ross WN. 1977. Optical recording of neuronal activity in an invertebrate central nervous system; simultaneous recording from several neurons. *J Neurophysiol* **40:** 1281–1291.

Salzberg BM, Obaid AL, Gainer H. 1986. Optical studies of excitation secretion at the vertebrate nerve terminal. *Soc Gen Physiol Ser* **40:** 133–164.

Seidemann E, Arieli A, Grinvald A, Slovin H. 2002. Dynamics of depolarization and hyperpolarization in the frontal cortex and saccade goal. *Science* **295:** 862–865.

Sharon D, Grinvald A. 2002. Dynamics and constancy in cortical spatiotemporal patterns of orientation processing. *Science* **295:** 512–515.

Shoham D, Ullman S, Grinvald A. 1991. Characterization of dynamic patterns of cortical activity by a small number of principal components. *Neuroscience* **17:** 1089.

Shoham D, Glaser DE, Arieli A, Kenet T, Wijnbergen C, Toledo Y, Hildesheim R, Grinvald A. 1999. Imaging cortical architecture and dynamics at high spatial and temporal resolution with new voltage-sensitive dyes. *Neuron* **24:** 791–802.

Siegel MS, Isacoff EY. 1997. A genetically encoded optical probe of membrane voltage. *Neuron* **19:** 735–741.

Slovin H, Arieli A, Hildesheim R, Grinvald A. 2002. Long-term voltage-sensitive dye imaging of cortical dynamics in the behaving monkey. *J Neurophysiol* **88:** 3421–3438.

Slovin H, Strick PL, Hildesheim R, Grinvald A. 2003. Voltage sensitive dye imaging in the motor cortex. I. Intra- and intercortical connectivity revealed by microstimulation in the awake monkey. *Soc Neuroci Abst* **554:** 8.

Spors H, Grinvald A. 2002. Temporal dynamics of odor representations and coding by the mammalian olfactory bulb. *Neuron* **34:** 1–20.

Sterkin A, Lampl I, Ferster D, Grinvald A, Arieli A. 1998. Real time optical imaging in cat visual cortex exhibits high similarity to intracellular activity. *Neurosci Lett* **51:** S41.

Stosiek C, Garaschuk O, Holthoff K, Konnerth A. 2003. In vivo two-photon calcium imaging of neuronal networks. *Proc Natl Acad Sci* **100:** 7319–7324.

Strick P, Grinvald A, Hildesheim R, Slovin H. 2003. Voltage sensitive dye imaging in the motor cortex II. Cortical correlates of Go/No-Go delayed response task. *Soc Neuroci Abst* **918:** 8.

Takashima I, Kajiwara R, Iijima T. 2001. Voltage-sensitive dye versus intrinsic signal optical imaging: Comparison of optically determined functional maps from rat barrel cortex. *Neuroreport* **12:** 2889–2894.

Tanifuji M, Yamanaka A, Sunaba R, Toyama K. 1993. Propagation of excitation in the visual cortex studies by the optical recording. *Jpn J Physiol* **43:** 57–59.

Tasaki I, Warashina A. 1976. Dye membrane interaction and its changes during nerve excitation. *Photochem Photobiol* **24:** 191–207.

Tasaki I, Watanabe A, Sandlin R, Carnay L. 1968. Changes in fluorescence, turbidity, and birefringence associated with nerve excitation. *Proc Natl Acad Sci* **61:** 883–888.

Toyama K, Tanifuji M. 1991. Seeing excitation propagation in visual cortical slices. *Biomed Res* **12:** 145–147.

Tsodyks M, Kenet T, Grinvald A, Arieli A. 1999. Linking spontaneous activity of single cortical neurons and the underlying global functional architecture. *Science* **286:** 1943–1946.

Vranesic I, Iijima T, Ichikawa M, Matsumoto G, Knopfel T. 1994. Signal transmission in the parallel fiber Purkinje-cell system visualized by high resolution imaging. *Proc Natl Acad Sci* **91:** 13014–13017.

Waggoner AS. 1979. Dye indicators of membrane potential. *Annu Rev Biophys Bioeng* **8:** 47–63.

Waggoner AS, Grinvald A. 1977. Mechanisms of rapid optical changes of potential sensitive dyes. *Ann N Y Acad Sci* **303:** 217–242.

Cite this introduction as *Cold Spring Harb Protoc;* doi:10.1101/pdb.top089367

Voltage-Sensitive Dye Imaging of Neocortical Activity

Amiram Grinvald, David B. Omer, Dahlia Sharon, Ivo Vanzetta and Rina Hildesheim

Cold Spring Harb Protoc; doi: 10.1101/pdb.top089367